JVSTA Journal of Vacuum Science & Technology A

Origin of defects on targets used to make extreme ultraviolet mask blanks

He Yu, Daniel Andruczyk, David N. Ruzic, Vibhu Jindal, and Patrick Kearney

Citation: Journal of Vacuum Science & Technology A **31**, 021403 (2013); doi: 10.1116/1.4788670
View online: http://dx.doi.org/10.1116/1.4788670
View Table of Contents: http://scitation.aip.org/content/avs/journal/jvsta/31/2?ver=pdfcov
Published by the AVS: Science & Technology of Materials, Interfaces, and Processing

Origin of defects on targets used to make extreme ultraviolet mask blanks

He Yu[a)]
Department of Nuclear, Plasma and Radiological Engineering, Center for Plasma Material Interaction, University of Illinois at Urbana-Champaign, Illinois 61801 and State Key Laboratory of Electronic Thin Films and Integrated Devices, School of Optoelectronic Information, University of Electronic Science and Technology of China, Chengdu 610054, People's Republic of China

Daniel Andruczyk and David N. Ruzic
Department of Nuclear, Plasma and Radiological Engineering, Center for Plasma Material Interaction, University of Illinois at Urbana-Champaign, Illinois 61801

Vibhu Jindal and Patrick Kearney
Sematech, Albany, New York, 12203

(Received 10 July 2012; accepted 28 December 2012; published 23 January 2013)

Particle formation is a major problem in extreme ultraviolet masks, and one source of these particles has been identified to be the targets used to produce the mask surfaces. In particular, the silicon (Si) and ruthenium (Ru) target appear to produce more particles, especially silicon. The evidence of this is seen as a rough region on the edges of the silicon target. The features in the region were found to be triangular mesas pointing in the direction of the incident beam. The aim of this research is to prevent the mesa formation features on the target and thus reduce particle formation on the target. Both Si and Ru targets were sputtered using different ion beam conditions to understand the mesa formation mechanisms on the target and explore the ion beam conditions that can mitigate mesas. A simple 2D Monte-Carlo computer model (Illinois surface analysis model) was used to understand the formation of mesas with different incident angles of ion beam (0°, 35°, 54°, 75°) that agrees with the shapes of mesas seen in the experiments. Additionally, SRIM was used to calculate sputtering yields to better understand the different mechanisms between Si and Ru. It is concluded from both experiment and calculation results that an effective way to stop mesas formation is to have a sample oscillating between 0° and the desired angle during sputtering.
 [http://dx.doi.org/10.1116/1.4788670]

I. INTRODUCTION

A. Background

Multilayer masks are key elements in the extreme ultraviolet (EUV) lithography process in the production of the next generation of microprocessors. They have high normal incidence reflectivity in the EUV spectral range and are the focusing and imaging components in EUV lithography.[1–5] A critical area in the production of these masks is the detection and reduction of defects on these masks[6] which can affect the whole production process. Particles are the largest source of defects in the production of these masks and originate from the targets that are used to sputter the different multilayers onto the mask substrate. In EUV lithography mask blank production, MoSi multilayers are deposited on top of a low thermal expansion material glass using an ion deposition technique. A 2.5-nm-thick Ru cap layer is deposited on top of the multilayer film to protect the multilayer film from exposure to harsh conditions during mask manufacturing.[7] In this ion deposition process, one source of particles is the silicon and ruthenium targets used to sputter material onto the multilayers. An example of a defect in the multilayer is shown in Fig. 1(a). In Fig. 1(b), energy dispersive x ray (EDX) and diffraction analysis of the particles show that the defect is primarily crystalline Si that originated from the target. It was observed that the periphery of the silicon target was rough and starting place of micron-scale mesas was on the surface. These features have been reported in the past by Tsong and Barber[8] who found hillock-like features on a silica glass surface due to argon bombardment and these features have also been described by Cong-Xin *et al.*[9] There are also a lot of groups working on pattern formation on surfaces by ion beam sputtering. Frost and Ziberi[10,11] studied the evolution of the surface topography of Si and Ge surfaces during low-energy ion-beam erosion. Gago *et al.*[12] reported that crystalline dots are produced on a Si (100) surface by low energy Ar^+ ion bombardment at normal incidence. Extensive progress has been made by Chan and Chason[13,14] in understanding the relationship among different kinetic regimes of sputter-induced pattern formation on surfaces. In this paper, the formation of mesas on both Si and Ru target surfaces during ion beam sputtering at different incident angles is analyzed experimentally as well as theoretically. Finally, a special design for mitigating formation of the mesas was included.

B. Formation of particle

Figure 2 shows scanning electron microscopy (SEM) of the observed hillocks on a silicon sample used in mask production by SEMATECH and also observed at the University of Illinois. The mesas have a few distinct features that are of interest. One is that the trailing edge of the mesa spreads out

a)Electronic mail: yuheuiuc@gmail.com

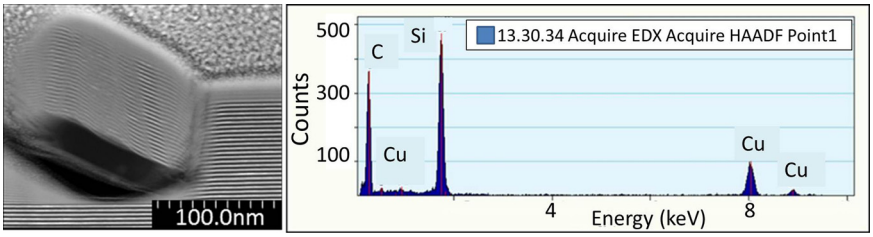

FIG. 1. (Color online) TEM (a) and EDX (b) analysis of a multilayer with Si defects (provided by SEMATECH).

in a fan shape in the direction of the beam. This fan shape has an origin where there possibly was a seeding feature on the surface. The leading edge which is exposed to the beam has a steep gradient. The difference in sputtering rate will eventually erode the surface while leaving the defect as a mesa that breaks off and runs to the substrate, finally makes the defect in the multilayers. Modeling shows that the sputtering yield at elevated angles is significantly higher than the yield at normal incidence. The edges of the rising mesa are sputtered away more slowly than the surrounding plane, making the mesa appear to be growing. The angular width of the mesa is determined by the angular spread of the ion beam. If that spread is large (as it is in the middle of the sputtered target), the feature will not appear, since ions coming from a variety of angles means that the difference in sputtering yield versus angle at a particular spot is significant. As is shown in Fig. 2(d), "L" is the length of the mesa. The size of the mesa depends on the beam angle. The larger the angle, the bigger L would be.

II. EXPERIMENT

The broad area ion-gun tool (BAIT) is used for the study of the surfaces. It consists of a vacuum chamber with a sample stand that is able to vary its angle from 0° to 90°. The sample stand can hold the target sample at one angle or vary the angle continuously between two angles for a defined time, for example, it can hold the sample at 0° for 5 s then at 54° for 5 s then back to 0° for 5 s, etc., for a set period of time. A VECCO 03FC ion gun with an Ion Tech., Inc. MPS-3000 FC controller produces an argon ion beam that is incident on the target surface. The beam can have an energy up to $E = 1200$ eV, but typical operating energy in this study is $E < 600$ eV since the ion beam at Sematech is run at 600 eV.[9] The angle of incidence used is $\theta = 54°$ since this is the angle that is used at Sematech as well. Every sample has been exposed to different angle beam for the same time period (6 h).

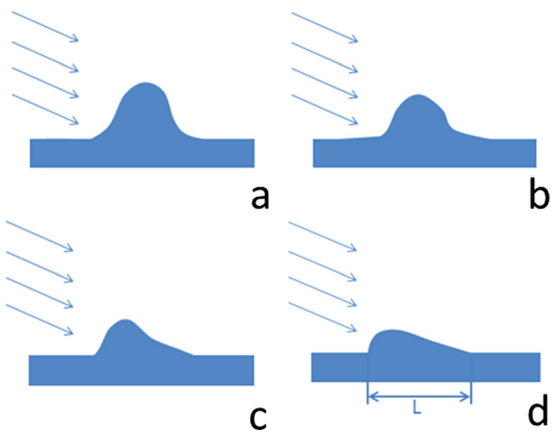

FIG. 2. (Color online) Process of mesa formation. Blue arrows indicate the direction of the beam. L is the length of "mesa." (a) Some initial imperfection on the surface. (b) The planar has been eroded, but the side of the feature facing the beam is not eroded as quickly, and the side being shadowed is not reduced at all. (c) A status before final shape has been formed (d) a mesa has risen out of the material with a trailing edge parallel to the beam direction.

A. Si

Figure 3 shows SEM images of samples taken from a silicon target. The samples were not polished, as shown in Fig. 3(a). Note the general shape of the mesas in Figs. 3(b)–3(d). They begin at a single point where the initial surface features occur and then fan out. Even though the ion beam is incident at an angle, θ, to the surface normal, which causes the sputtering, it still can have an angular spread around the starting point, which results in the fan shape. Several angles were used on crystalline Si samples to study formation of these features. The first angle studied, 35°, produced mesas that were between 2 and 5 μm wide, as shown in Fig. 3(b). Using a 54° incident angle beam produced mesas all over the surface. As shown in Fig. 3(c), the mesas are around 8–9 μm wide and 11–12 μm long. If the beam angle is increased to 75°, the mesas became larger, 10 μm wide and 16 μm long, as seen in Fig. 3(d). Clearly, the general shape and size of the mesas is dependent on the angle. The larger the angle, the longer the features and the sharper the leading edge is.

B. Ru

Figure 4(a) shows an unpolished Ru sample surface with some Si impurities. When a 35° beam was used to sputter the surface, mesa features became apparent. This is shown in Fig. 4(b). However, these features were not found in the other area, suggesting that the mesas originate from a Si impurity. When the beam angle is increased from 35° to 54°, many more mesas were formed. Compared with Si, the Ru mesas are around only 100 nm long. Besides, $Y(\theta, E)/Y(0, E)$ is the proportion of sputtering yield at θ angle and sputtering yield at normal incidence. This value shows how easy it is for mesas to form on the target during sputtering. For Ru, 54° has much higher $Y(\theta, E)/Y(0, E)$ values, which can easily

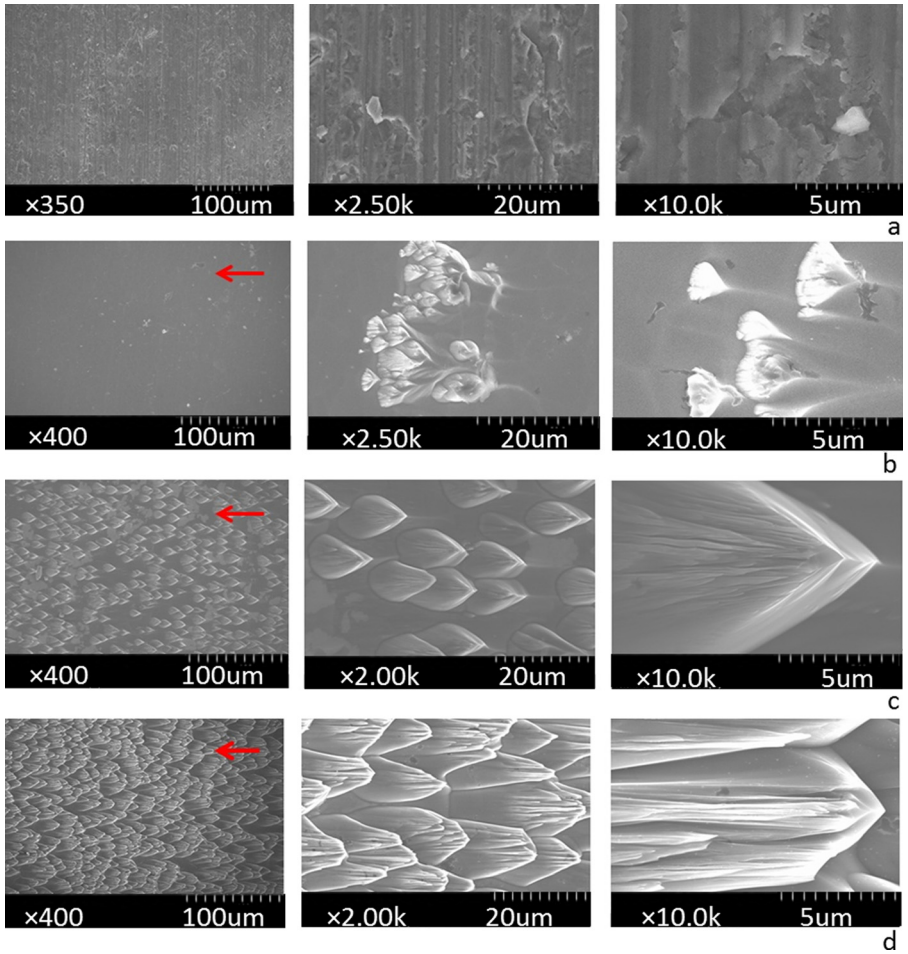

FIG. 3. (Color online) SEM images of samples (100, 20, and 5 μm resolution) taken from sintered silicon target produced by the BAIT. The arrow indicates the direction of the beam. (a) Unsputtered sintered Si surface. (b) Beam conditions were E = 600 eV, $\theta = 35°$ exposed for t = 6 h. (c) Beam conditions were E = 600 eV, $\theta = 54°$ exposed for t = 6 h. (d) Beam conditions were E = 600 eV, $\theta = 75°$ exposed for t = 6 h. The arrow indicates the direction of the beam.

form these mesas predicted through theoretical analysis (shown in theoretical analysis section). At 75°, the number of mesas is not so high as at 54°.

C. Mitigating formation of mesas

From the previous study, we notice that these mesas can be reduced by reducing the beam angle. When 0° incident angle was used for the beam to clean the Si surface for 6 h, an interesting feature was found. The surface is basically smooth, devoid of any mesas but there is an occasional "spike," as shown in Fig. 5(a). It represents an intermediate phase in the mesas being sputtered away. This spike shape mesa was also predicted by our 2D Monte-Carlo computer modeling that will be shown in the theoretical analysis section.

In lieu of the data in Sec. II B, it can be seen that the best way to remove the mesas would be by having the surface vary between two incident angles. Figure 6 is the time series used to remove the mesa features. One of these angles needs to be at 0° or as close to it. The surface would initially be used at the desired angle and then be exposed to a beam that is normal to the surface, ensuring that the mesas are sputtered away.

A special design was explored by having the Si surface exposed to an incident beam of 0° and 54° every 5–6 s. The Si sample was sputtered for 6 h. It showed that the surface was cleaned of the majority of surface roughness, shown in Fig. 7. The features seen in Fig. 3 are not present. There are still few features present and these would need more time to be sputtered away. However, this shows that an effective way without too much modification to the system to stop particle formation is to have a sample oscillating between 0° and the desired angle. It is important to note that the piece of mesa on the target will break off instead of going to the substrate in one piece. So our method does not reduce the defects size on the masks. It will reduce the chance of defects happening however.

III. THEORETICAL ANALYSIS

A. Sputtering yields

A stopping range of ions in matter (SRIM) code[15–17] is used to determine the sputtering yield, *Y*. This is a well-developed code that is readily available and is based on the TRIM code. SRIM is used to find the sputtering yields of an argon ion incident on a silicon surface for different incident angles and ion energies. In Fig. 8, sputtering yield was

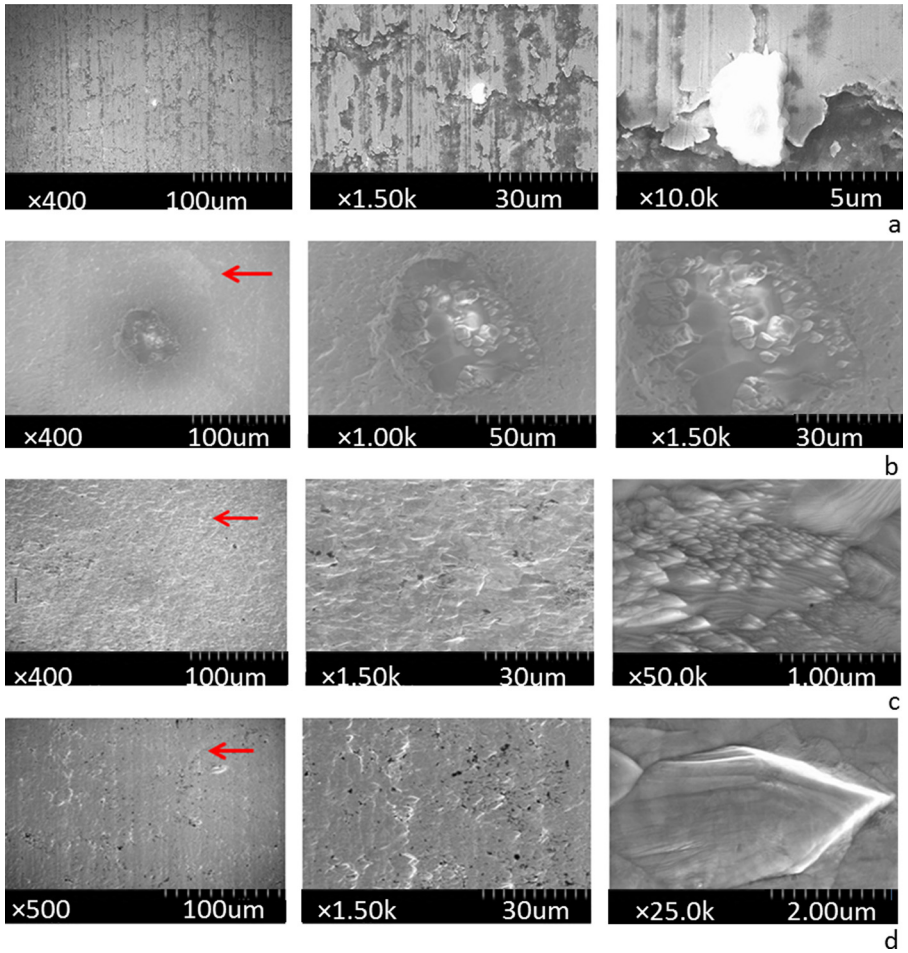

FIG. 4. (Color online) SEM images of samples taken from Ru target produced by the BAIT. The arrow indicates the direction of the beam. (a) Unsputtered Ru target surface. (b) Beam conditions were E = 600 eV, $\theta = 35°$ exposed for t = 6 h. (c) Beam conditions were E = 600 eV, $\theta = 54°$ exposed for t = 6 h. (d) Beam conditions were E = 600 eV, $\theta = 75°$ exposed for t = 6 h.

calculated for silicon and ruthenium using angles from 0° to 90° and beam energies from 50 to 1200 eV.

The sputtering yield of Si and Ru bombarded with argon are shown in the Figs. 8(a) and 8(b), respectively. The maximum sputtering yield for Si is at 75°, with a yield of $Y = 4.5$ atoms/ion at an energy of 1.2 keV. The difference in sputtering yield between 0° and peak (75°) is about 4.0, which is very high. Compared with Si, Ru has much more uniform sputtering yield value. It seems that the maximum sputtering yield for Ru is not 75°, but 55°–65°, depending on the energy. In Figs. 8(c) and 8(d), the parameter of $Y(\theta, E)/Y(0, E)$ shows how easy it is for mesas to form on the target during sputtering. The higher this value, the easier features form which could lead to particle formation. Because in Si this parameter has a much higher value, more particles originate from the Si target than the Ru; this is also the reason why the size of mesas on the Si target is much bigger than the ones on the Ru target in the experiment.

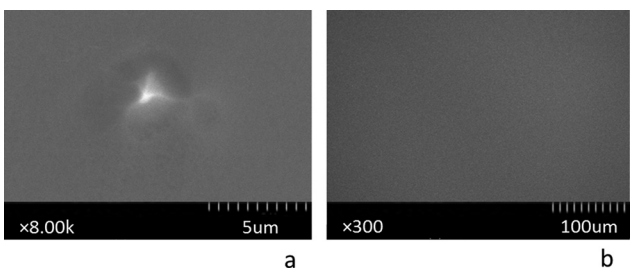

FIG. 5. Surface feature at 0° incident. (a) A spike feature which is an intermediate step in the particle being sputtered away and (b) the smooth surface that is obtained from exposure to a 0° incidence beam for 6 h.

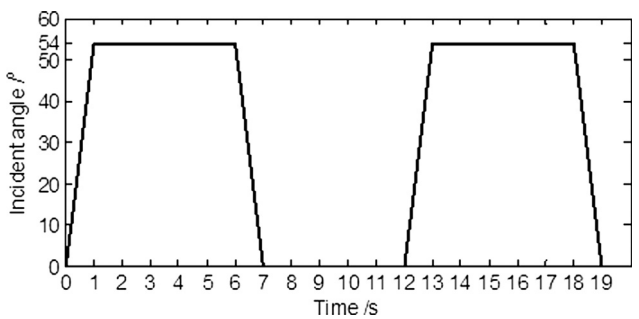

FIG. 6. Time series used to remove the mesas.

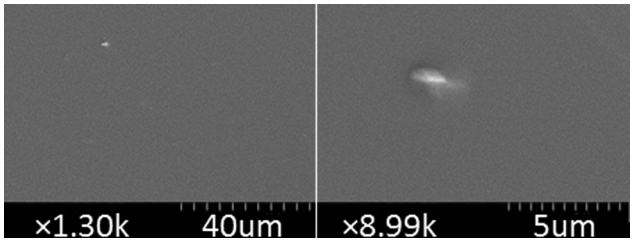

FIG. 7. SEM of a sample that has been run alternating between 0° and 54° for 6 h. There are still two larger features that would need more time to also be removed. The arrow indicates the beam direction.

For Si, the maximum value of $Y(\theta, E)/Y(0, E)$ is at 75°. However, the maximum of this parameter for the Ru target is at 54° instead of at 75° when the beam energy is 600 eV (beam condition in the experiment). From SEM images,the 54° beam can produce mesas more easily on Ru surface. Additionally, for Si, the beam energy does not impact particle formation. Particle formation is related to the mesa formation but may not competely depend on the formation dynamics alone. Since Si is a single crystal, the features that do form are still quite connected to the surface. For Ru, the material is polycrystalline, so when the sizes of the mesas are very small, and the surroundings are sputtered down below a grain boundary, the particle could detach. These yields are used in the following 2D Monte-Carlo modeling.

B. 2D Monte-Carlo computer model

The Illinois surface analysis model (iSAM) is a Monte-Carlo based Ray Tracing computer model that has been written to help understanding in the growth of the mesas. The sputtering yield we simulated previously was used to calculate the sputtered layer with different incident angle at different position on the target. The modeling shows that the mesas have a level of shielding, which forms a ramp on the trailing edge of the mesas at the angle of the incident beam. At 35°, we see the structures where there is the sharp leading edge as well as a sharp trailing edge, shown in Fig. 9(a). At 54°, Fig. 9(b) shows the pronounced steep leading edge that is facing the direction the ion beam is coming from, but the trailing edge of the beam is rounded. At 75°, the mesa features are even rounder. The shadowing effect of the initial feature is very pronounced and the trailing edge is quite elongated and at the angle of the ion beam. It shows the leading edge is not as steep as in the previous angles due to the sputtering being a lot less at the local angle than it would have been at the other angles. By growing in size, the mesas also started to overlap with each other and all of these simulation results are seen quite vividly in experiments of Si samples. Finally, we simulated the mesa formation at 0°. Fig. 9(d) shows an intermediate step where a spire is produced from a surface feature. This was seen experimentally as

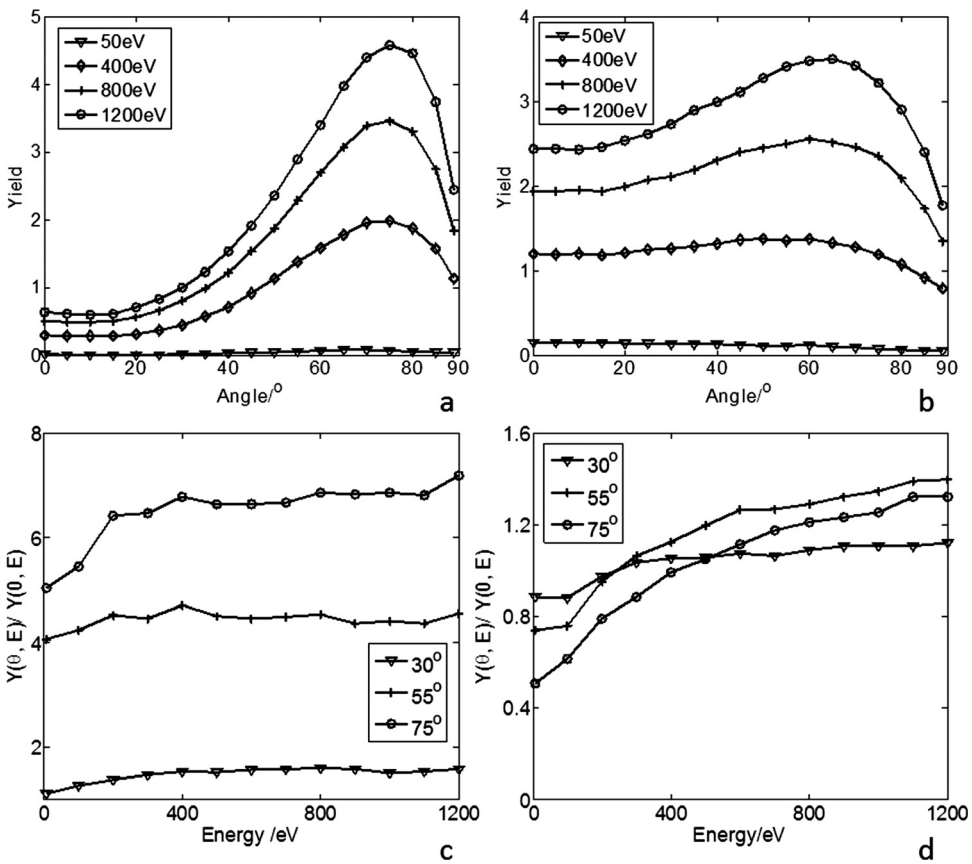

FIG. 8. Calculation results of SRIM software. Note different verticle scales. The differential sputtering yield of Si is much more pronounced than that of Ru. (a) Calculation of Ar on Si sputtering yield vs energy and angle. (b) Calculation of Ar on Ru sputtering yield vs energy and angle. (c) Calculation of $Y(\theta, E)/Y(0, E)$ of Si vs energy. (d) Calculation of $Y(\theta, E)/Y(0, E)$ of Ru vs energy.

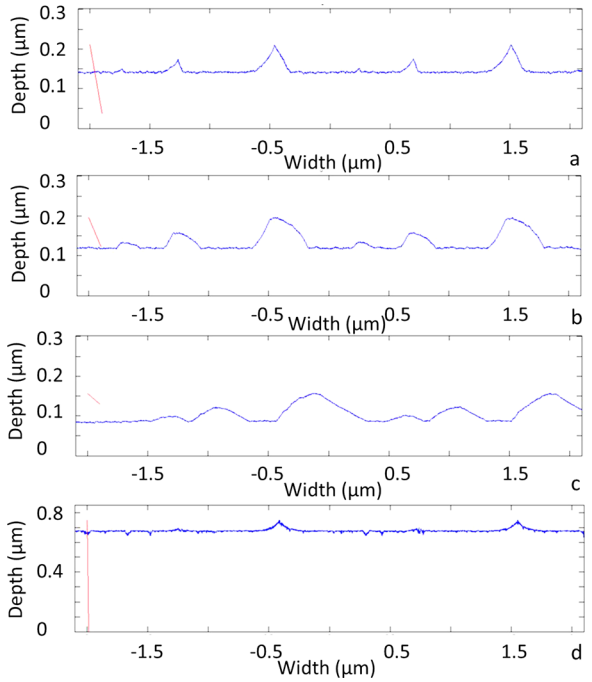

FIG. 9. (Color online) 2D Monte-Carlo simulation of mesa formation at 35°, 54°, 75°, and 0°, respectively. (a) At 35°, the features are very sharp and pointed. The mesas are already starting to become quite defined. (b) Simulated features at 54° showing the much more rounded trailing edge, while the leading edge is still steep. The farthest part of the trailing edge is due to shadowing effects and comes in at 54° which can be compared with the red line on the left, which is showing the angle the beam is incident at. (c) Simulated mesas at 75°. These show the elongated structures that are seen in SEMs, and the leading edges are not as steep as seen previously. (d) Simulated mesas at 0°. This is an intermediate step toward sputtering a surface clean.

shown in Fig. 5 and validates the spire like surface seen in the simulation.

IV. CONCLUSION

Mesas have been observed on targets used in the production of EUV masks. These eventually can form particles that are sputtered off the target surface and land on the mask substrate surface and can form imperfection in the mask. Mesa formation seen on the surface of both Si targets and Ru targets was analyzed experimentally as well as theoretically and simulated using a Monte-Carlo program (iSAM). Experiment of both Si and Ru targets sputtered by angles of 0°, 35°, 54°, 75° has been done. SRIM was used to calculate the sputtering yields for Si and Ru to better understand the mechanisms behind the sputtering and mesa formation. Moreover, a simple Monte-Carlo computer model has been written to help understand the growth of the mesas. The Monte-Carlo simulation agrees with the general shape of the mesas with different angles, indicating that their mechanism of formation is correct.

The formation of mesas largely depends on the angle at which the ion beam is incident on the surface. At 35°, few particles are likely to be formed. Beyond about 35°, surface features start to form that eventually lead to particles on the Si target. As the angle increased, more particles are formed. It is observed that mesas are longer and originate from a sharper point before melding into the surface. In the calculation section, the parameter of $Y(\theta, E)/Y(0, E)$ was calculated by SRIM. This value shows how easy it is for mesas to form on the target during sputtering. This value is increased by increasing the angle of the beam. That is why more mesas are formed when we increased angle in the experiment. For Ru, many mesas are grown from Si impurities when the surface is sputtered by a 35° beam. However, these features are not found in other areas. This agrees with the calculation results as well. Because in Si $Y(\theta, E)/Y(0, E)$ has a much higher value, more particles originate from the Si target than the Ru. Furthmore for Ru, when the angle is increased from 35° to 54°, the value of $Y(\theta, E)/Y(0, E)$ is going up. In the experiment, when the beam angle is increased to 54°, many small (i.e., 100 nm long) mesas are produced. Finally, we came to the conclusion from both experiment and calculation results that an effective way to stop mesas formation is to have a sample oscillating between 0° and the desired angle. Modeling and experiments have shown that this is an effective way to stop the mesa features from forming and thus any precursor for a particle that can become a contaminant on the mask.

ACKNOWLEDGMENTS

The authors would like to acknowledge SEMATECH contract: Agreement 402106NY, Mod 3, Project LITH184 which has supported this work. Also thanks to Professor Y. Jiang, State Key Laboratory of Electronic Thin Film and Integrated Devices, School of Optoelectronic Information, University of Electronic Science and Technology of China, Chengdu 610054, People's Republic of China, for student support.

[1]T. Chasse *et al.*, Vac. **71**, 407 (2003).
[2]D. Y. Kim, H. J. Lee, H. Y. Jung, and N.-E. Lee, J. Vac. Sci. Technol. A **26**, 857 (2008).
[3]Y. R. Park, J. H. Ahn, J. S. Kim, B. S. Kwon, and N.-E. Lee, J. Vac. Sci. Technol. A **28**, 761 (2010).
[4]V. Jindal, C. C. Lin, J. Harris-Jones, and J. Kageyama, Proc. SPIE **7969**, 79691A_1 (2011).
[5]S. Bajt, J. Vac. Sci. Technol. A **18**, 557 (2000).
[6]H. Yun, F. Goodwin, S. Huh, K. Orvek, B. Cha, A. Rastegar, and P. Kearney, Proc. SPIE **7379**, 73790G (2009).
[7]A. Rastegar and V. Jindal, Proc. SPIE **8352**, 83520W (2012).
[8]Tsong and D. J. Barber, J. Mater. Sci. **7**, 687 (1972).
[9]C. Ren, G. Chen, X. Fu, J. Yang, H. Fang, and S. Tsou, Radiat. Eff. **77**, 177 (1983).
[10]B. Ziberi, M. Cornejo, F. Frost, and B. Rauschenbach, J. Phys.: Condens. Matter **21**, 224003 (2009).
[11]F. Frost, R. Fechner, B. Ziberi, J. Vollner, D. Flamm, and A. Schindler, J. Phys.: Condens. Matter **21**, 224026 (2009).
[12]R. Gago, L. Vazquez, R. Cuerno, M. Varela, and C. Ballesteros, Appl. Phys. Lett. **78**, 3316 (2001).
[13]W. L. Chan and E. Chason, J. Appl. Phys. **101**, 121301 (2007).
[14]E. Chason and W. L. Chan, Top. Appl. Phys. **116**, 53 (2010).
[15]C. C. Walton, P. A. Kearney, P. B. Mirkarimi, J. M. Bowers, C. Cerjan, A. L. Warrick, K. Wilhelmsen, E. Fought, and C. Moore, Proc. SPIE **3997**, 496 (2000).
[16]See www.srim.org/SRIM/SRIM2006.htm for SRIM (2006).
[17]J. F. Ziegler, J. P. Biersack, and U. Littmark, *The Stopping and Range of Ions in Solids* (Pergamon, New York, 1985).